nature geoscience

Brief Communication

https://doi.org/10.1038/s41561-023-01202-6

Mid-Proterozoic day length stalled by tidal resonance

Received: 13 June 2022

Accepted: 12 May 2023

Published online: 12 June 2023

Check for updates

Ross N. Mitchell [1,2] ✉ & Uwe Kirscher [3,4]

We present statistical analysis of a compilation of observational constraints on the Precambrian length of day and find that the day length stalled at about 19 h for about 1 billion years during the mid-Proterozoic. We suggest that the accelerative torque of atmospheric thermal tides from solar energy balanced the decelerative torque of lunar oceanic tides, temporarily stabilizing Earth's rotation. This stalling coincides with a period of relatively limited biological evolution known as the boring billion.

Tidal forces of an orbiting satellite control the evolution of a planet's rotation[1,2]. Because Earth rotates faster than the orbital angular velocity of the Moon, Earth's oceanic tidal bulge is pushed ahead of the Moon. This offset exerts a torque on the Moon, which—transferring angular momentum from Earth to the Moon—boosts the Moon to a farther orbit and slows Earth's rotation, increasing its length of day (LOD) over time. Theoretical lunar recession models have generally been characterized by a steady trend over the past 3 or 4 billion years[3–5]. In contrast with traditional models that propose continuously evolving conditions is the speculation of a temporarily long time interval of constant day length during Precambrian time potentially arising from a stabilization due to resonance with the atmospheric thermal tide[6–8]. There is therefore a need for a sufficiently abundant number of Precambrian LOD constraints that can be used to further understand the evolution of the Earth–Moon system in high temporal resolution.

In contrast with their oceanic counterpart gravitationally excited by the pull of the Moon, atmospheric tides are thermally excited by the absorption of sunlight by water vapour and ozone, the largest of which is semidiurnal. Due to the arrangement of the three-body system and Earth's sense of rotation, the lunar semidiurnal oceanic tide applies a decelerative torque and the solar semidiurnal atmospheric tide applies an accelerative torque on Earth's rate of rotation (Fig. 1). A resonance-stabilized day length is the unique condition where, at the point of resonance, the lunar oceanic torque can be cancelled by the solar atmospheric torque. This might have been possible in the Precambrian when the lunar torque is thought to have been one-fourth of its present value due to weaker frictional coupling between Earth and the Moon at faster palaeorotation[4,6,7]. If the opposing atmospheric torque became equal to the diminished lunar torque, Earth's long-term rotational deceleration could have been temporarily halted at a constant day length for some interval of Precambrian time[6].

The geological record has multiple means of preserving an archive of LOD over time and, by inference, the history of Earth–Moon distance. Biologically mediated means of recording LOD, such as tree rings and coral growth bands, preserve reliable annual banding, but are restricted to the Phanerozoic eon, since 539 million years ago (Ma), when animal life evolved[9]. For Precambrian time, before the Phanerozoic, other LOD records must be used. When the resonance-stabilized day length hypothesis was first proposed, only a small handful of Precambrian LOD constraints were available. These came from the seasonal sinusoidal growth of stromatolites (following the annual Sun angle), but such constraints require high sediment accumulation rates, which are rare in such depositional settings. The only other constraints at the time came from tidal rhythmites, but such depositional settings are rarely preserved and/or are difficult to prove in the absence of independent geochronology, which is often lacking in Precambrian successions. For example, conflicting interpretations of LOD have been attained for the tidal rhythmites of the ~900 Ma Big Cottonwood Formation[10,11].

Critically, LOD can also be calculated from cyclostratigraphic studies of Milankovitch orbital cycles because the astronomical precession frequency (k) is a function of Earth's rotation rate[12]. This study was prompted by a recent proliferation of new cyclostratigraphic-based LOD constraints having become available for the Precambrian, with 12 of the 22 Precambrian LOD constraints having been generated in the past 7 years (Extended Data Table 1). Our statistical change-point analysis of the most recent, much more abundant Precambrian LOD compilation indeed yields, as theorized, a flatlining of day length between 2 and 1 billion years ago (Ga) during the mid-Proterozoic (Fig. 2). This observation thus empirically vindicates the modelling-based

[1]State Key Laboratory of Lithospheric Evolution, Institute of Geology and Geophysics, Chinese Academy of Sciences, Beijing, China. [2]College of Earth and Planetary Sciences, University of Chinese Academy of Sciences, Beijing, China. [3]Department of Geosciences, University of Tübingen, Tübingen, Germany. [4]Earth Dynamics Research Group, The Institute for Geoscience Research, School of Earth and Planetary Sciences, Curtin University, Perth, Western Australia, Australia. ✉e-mail: ross.mitchell@mail.iggcas.ac.cn

https://doi.org/10.1038/s41561-023-01202-6

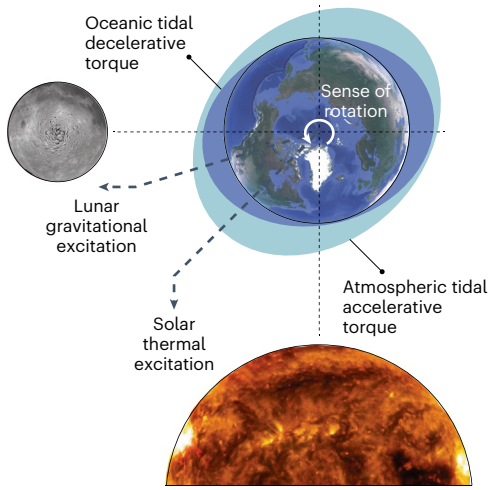

Fig. 1 | Opposing torques of semidiurnal oceanic and atmospheric tides acting on Earth's rotation. At the point of resonance, the oceanic and atmospheric tidal torques would balance, stabilizing Earth's rotation rate at a constant day length. The images are not to scale. Figure adapted with permission from ref. 6, Elsevier. Earth and Moon images were generated using GoogleEarth. Earth data/image sources: data (SIO, NOAA, U.S. Navy, NGA, GEBCO) and image (Landsat/Coperincus and IBCAO) and Moon image source: NASA/USGS/JAXA/SELENE. Sun image is from NASA/SDO.

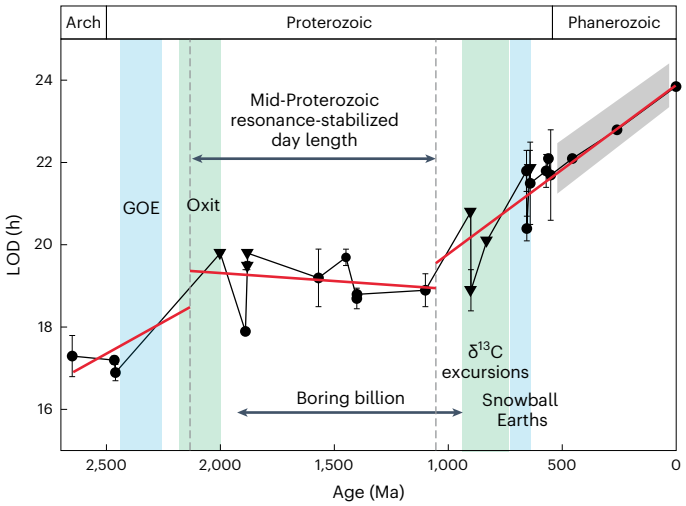

Fig. 2 | Precambrian LOD constraints and trends. The LOD compilation is detailed in the Methods and provided in Extended Data Table 1. Following ref. 21, LOD error bars are defined by the difference between the average of all precession/obliquity-based LOD estimates for a rock unit and the estimate with the largest difference from the mean. The red linear regressions were automatically assigned by the change-point algorithm without any a priori data binning (Methods). The grey band encapsulates numerous Phanerozoic LOD constraints[9], with two recent cyclostratigraphic constraints from the Palaeozoic[19] and the present day length shown. Non-cyclostratigraphic constraints from tidal rhythmites and stromatolites (triangles) with fine-scale layering possibly containing cryptic discontinuities may represent maximum LOD estimates[18,22]. Some data lack uncertainties because insufficient information was provided in the original studies (a sensitivity test is provided in Extended Data Fig. 1). Arch, Archaean; $\delta^{13}C$, carbon isotope.

hypothesis of the emergence of resonance between oceanic (lunar) and atmospheric (solar) tides acting on Earth's rotation during the Precambrian[6,7].

Naturally, when data and theory are compared, even when there is general agreement, there is also something that can be learned from the slight mismatch. Given their vertical wavelength, atmospheric tides (also known as Lamb waves) are measurable phenomena in Earth's atmosphere, with a 10.4-h period in the present atmosphere[13]. Hypotheses for the potential for a Precambrian resonance-stabilized day length[6,7] have previously assumed that atmospheric tides have always had a constant 21-h period (~10.5-h resonance). However, the Precambrian LOD data indicate a shorter ~19-h period (~9.5-h resonance). There is uncertainty in the ~19-h estimate from several sources, including uncertainties in each of the LOD estimates, differences in the methods used to estimate LOD and still a limited number of Precambrian LOD data, particularly spanning the critical Proterozoic interval. A mid-Proterozoic flatlining is well supported by five modern cyclostratigraphic constraints with relatively small uncertainties, but more such studies have to be conducted to further test and more accurately determine the resonance period. As the LOD data indicate that the putative resonance would have been achieved sometime between 2.46 and 2.00 Ga, the question then becomes whether the atmospheric conditions during this time were amenable to Lamb waves being ~10% faster than they are today.

The stabilizing of day length appears to have occurred shortly after two of the most notable fluctuations in atmospheric conditions that may have caused a fundamental change in the atmospheric tide, thus inducing resonance with the oceanic tide. These two intervals—the Great Oxidation Event[14] (GOE) and the exit from oxygen[15] (Oxit)—stand in stark contrast, with the GOE representing the addition of oxygen and Oxit its subtraction. Only low oxygen levels, plus hotter temperatures, relative to today may make Lamb waves the requisite 10% faster than they are today, approaching the ~19-h mid-Proterozoic day length observed (Fig. 3 of ref. 6). Furthermore, as the absorption of sunlight by ozone occurs at both great depths and higher altitudes than that of water vapour, ozone is more important in the excitation of atmospheric tides[16]; thus, its accumulation following the GOE (by O_2 molecules being photolysed by ultraviolet radiation and recombining with O atoms to create O_3) could have sufficiently increased the magnitude of the opposing solar tide to rival that of the smaller Precambrian lunar tide, thereby stabilizing LOD. Therefore, the succession of the GOE creating an ozone layer and the Oxit then decreasing oxygen levels may have played iterative roles in Earth entering resonance, with the most plausible surface temperatures at a resonance of ~19 h of day length being achieved with reduced O_2 and modern O_3 (ref. 6). The warm surface temperatures implied by such a model may have been achieved by the reduced O_2 following Oxit having caused surface warming[17]. There are multiple possible explanations for how escape from the resonance might have occurred[6,7]. Based on timing, this was probably somehow related to changes in atmospheric temperature or composition during the onset of severe climatic variability in the Neoproterozoic (Fig. 2).

Day length remaining constant at ~19 h for 1 billion years carries implications for the Earth–Moon system, as well as for Earth history. One consequence would be an increase in the angular momentum of the overall Earth–Moon system due to the extraction of additional angular momentum from Earth's orbit during the resonance[6]. One current limitation is that cyclostratigraphic studies assume conservation of angular momentum when converting from k to LOD[18,19]; therefore, proposals should be considered for how to estimate LOD without such an assumption. On Earth, the prolonged interval of stalled day length corresponds closely with the interval of similarly stalled biologic evolution, and geochemical and tectonic quiescence known as the boring billion (Fig. 2). Tectonically, temporal changes in the kinetic energy of rotation due to LOD can be mechanistically considered a contributing force to energies required to power plate tectonics[20]. Biologically, our work is consistent with the idea[8] that both the delayed rise of photosynthetically produced atmospheric oxygen and the rise of complex life, both which occurred only late in the Neoproterozoic, were delayed until the resonance was broken and longer days could provide photosynthetic

bacteria with sufficient sunlight to raise oxygen levels high enough to support large Metazoan life.

Online content

Any methods, additional references, Nature Portfolio reporting summaries, source data, extended data, supplementary information, acknowledgements, peer review information; details of author contributions and competing interests; and statements of data and code availability are available at https://doi.org/10.1038/s41561-023-01202-6.

References

1. Darwin, G. A tidal theory of the evolution of satellites. *Observatory* **3**, 79–84 (1879).
2. Darwin, G. On the secular changes in the elements of the orbit of a satellite revolving about a planet distorted by tides. *Nature* **21**, 235–237 (1880).
3. Webb, D. J. Tides and the evolution of the Earth–Moon system. *Geophys. J. Int.* **70**, 261–271 (1982).
4. Hansen, K. S. Secular effects of oceanic tidal dissipation on the Moon's orbit and the Earth's rotation. *Rev. Geophys.* **20**, 457–480 (1982).
5. Green, J. A. M., Huber, M., Waltham, D., Buzan, J. & Wells, M. Explicitly modelled deep-time tidal dissipation and its implication for Lunar history. *Earth Planet. Sci. Lett.* **461**, 46–53 (2017).
6. Zahnle, K. & Walker, J. C. G. A constant daylength during the Precambrian era? *Precambrian Res.* **37**, 95–105 (1987).
7. Bartlett, B. C. & Stevenson, D. J. Analysis of a Precambrian resonance-stabilized day length. *Geophys. Res. Lett.* **43**, 5716–5724 (2016).
8. Klatt, J. M., Chennu, A., Arbic, B. K., Biddanda, B. A. & Dick, G. J. Possible link between Earth's rotation rate and oxygenation. *Nat. Geosci.* **14**, 564–570 (2021).
9. Williams, G. E. Geological constraints on the Precambrian history of Earth's rotation. *Rev. Geophys.* **38**, 37–59 (2000).
10. Sonett, C. & Chan, M. A. Neoproterozoic Earth–Moon dynamics: rework of the 900 Ma Big Cottonwood Canyon tidal laminae. *Geophys. Res. Lett.* **25**, 539–542 (1998).
11. Sonett, C., Zakharian, A. & Kvale, E. Ancient tides and length of day: correction. *Science* **274**, 1068–1069 (1996).
12. Berger, A. & Loutre, M. F. Astronomical forcing through geological time. *Spec. Publ. Int. Assoc. Sedimentol.* **19**, 15–24 (1994).
13. Kovalam, S. & Vincent, R. A. Intradiurnal wind variations in the midlatitude and high-latitude mesosphere and lower thermosphere. *J. Geophys. Res. Atmos.* **108**, 4135 (2003).
14. Lyons, T. W., Reinhard, C. T. & Planavsky, N. J. The rise of oxygen in Earth's early ocean and atmosphere. *Nature* **506**, 307–315 (2014).
15. Hodgskiss, M. S. W., Crockford, P. W., Peng, Y., Wing, B. A. & Horner, T. J. A productivity collapse to end Earth's Great Oxidation. *Proc. Natl Acad. Sci. USA* **116**, 17207–17212 (2019).
16. Lindzen, R. S. & Chapman, S. Atmospheric tides. *Space Sci. Rev.* **10**, 3–188 (1969).
17. Poulsen, C. J., Tabor, C. & White, J. D. Long-term climate forcing by atmospheric oxygen concentrations. *Science* **348**, 1238–1241 (2015).
18. Meyers, S. R. & Malinverno, A. Proterozoic Milankovitch cycles and the history of the solar system. *Proc. Natl Acad. Sci. USA* **115**, 6363–6368 (2018).
19. Zhou, M. et al. Empirical reconstruction of Earth–Moon and solar system dynamical parameters for the past 2.5 billion years from cyclostratigraphy. *Geophys. Res. Lett.* **49**, e98304 (2022).
20. Varga, P. & Fodor, C. About the energy and age of the plate tectonics. *Terra Nova* **33**, 332–338 (2021).
21. Bao, X. et al. Length of day at c. 1.1 Ga based on cyclostratigraphic analyses of the Nanfen Formation in the North China craton, and its geodynamic implications. *J. Geol. Soc.* **180**, jgs2022-022 (2022).
22. Lantink, M. L., Davies, J. H. F. L., Ovtcharova, M. & Hilgen, F. J. Milankovitch cycle constraints on the Earth–Moon system 2.46 billion years ago. *Proc. Natl Acad. Sci. USA* **119**, e2117146119 (2022).

Methods

Precambrian LOD constraints

LOD constraints from Precambrian time are compiled in Extended Data Table 1 Refs. 30–43. A recent compilation of Precambrian LOD constraints[21] provided a basis for our compilation. Additions to and exclusions from the LOD compilation of ref. 21 are discussed.

The ~2,450 Ma Weeli Wolli Formation of the Pilbara craton of Western Australia has yielded two tidalite-based LOD estimates (17.1 ± 1.1 and 18.8 ± 0.6 h) based on different tidal interpretations of the same layering[9,23], one of which must be incorrect, and no independent constraint on sedimentation is available. As we were unable to pick between them, and since a reliable cyclostratigraphic study[24] of the underlying and only slightly older ~2,460 Ma Joffre Member of the Brockman Iron Formation recently became available to use instead for this age, we excluded the ambiguous estimates from the Weeli Wolli Formation. Also in Pilbara, the ~2,465 Ma Dales Gorge Member of the Brockman Iron Formation directly underlying the Joffre Member was studied by ref. 25, and its LOD estimate, including uncertainty, has been updated by ref. 19. Ref. 19 also provides an additional LOD estimate for the ~655 Ma Datangpo Formation of South China. An oldest LOD estimate at ~3.2 Ga comes from the Moodies Group tidal rhythmites of the Barberton Greenstone Belt of Kaapvaal craton in South Africa, but is typically excluded from most compilations[18,19,21] due to the ambiguities detailed in ref. 24, and is also excluded here. A LOD estimate from the ~1,450 Ma Hongshuizhuang Formation of North China[26], overlooked by the compilation of ref. 21, is included here.

One additional constraint not included in previous compilation comes from the ~1,890 Ma Rocknest Formation[27,28] from the Coronation Basin of Wopmay Orogen of the Slave craton. Multiple stratigraphic sections of the carbonate parasequences were measured along strike and in great detail. Two scales of cyclicity were identified: a high-frequency bandwidth with parasequence cycles of an average thickness of 10 m; and grand cycles of 75–100 m. Interpreting the former as precession and the latter as short eccentricity (consistent with independent geochronological estimates of the sediment accumulation rate) yields a bundling of ~8.75 precession cycles per short eccentricity cycle. Assuming that the eccentricity metronome is more or less stable through geologic time[29] and taking the arithmetic mean of 109.4 thousand years (kyr) of the two strongest components of short eccentricity (94.9 and 123.9 kyr) thus yields a period for precession at this age of 12.5 kyr. As only one average bandwidth of precession is identified (of the five main components of the climatic precession index), we convert to LOD for both the shortest and the longest precessional components (LOD = 17.30 and 18.41 h, respectively) and take the average of this range (LOD = 17.9 h).

Using all of the identified obliquity and precession periods to calculate LODs, ref. 21 regards the mean value of the largest and smallest values as the LOD and the difference between the average and the largest value as the uncertainty. A MATLAB script modified from ref. 21 for converting measured Milankovitch periods of precession and/or obliquity to LOD is provided online. See also refs. 18,19 for further discussion on how climatic precession, which is measured by cyclostratigraphy and is derived from the fundamental frequencies associated with the orbits of the five innermost planets and the precession constant k, is used to constrain LOD. In light of our evidence for LOD stabilization, however, the conventional approach may be insufficient. Conversion of cyclostratigraphy-based k to LOD assumes conservation of angular momentum in the Earth–Moon system. However, constant day length invalidates this assumption, where there would be an increase in the angular momentum of the Earth–Moon system during the period of resonance. Zahnle and Walker[6] estimated that this increase in angular momentum being extracted from Earth's orbit would be 10–20% over the lifetime of the solar system. Therefore, over the ~1 billion year-long resonance interval, the increase was probably «10%. Nonetheless, whether this increase is still potentially large enough not to be negligible should be considered in future work.

Change-point analysis

The MATLAB algorithm findchangepts was used to conduct a change-point analysis[30,31] and detect any abrupt changes in LOD signal. Lines of free slopes and ages of change points were automatically assigned by the algorithm without any user input. The number of change points and their associated slopes are defined such that the sum of the residual error is minimized.

The statistical resampling approach shown in Extended Data Fig. 1 was next used to test the robustness of our results. For LOD estimates without associated estimates of uncertainty, an error of 1 h was assigned related to the largest observed uncertainties. Then, each error was used as standard deviation in a normally distributed random value that was added (subtracted) to each respective LOD value. This resampling was done 1,000 times. For each of the 1,000 repetitions, the findchangepts analysis was carried out. To investigate the stability of the middle interval of the LOD evolution, all linear regression lines of the middle interval of the 1,000 analyses were plotted and a mean slope of all regression lines was calculated. We also plot a histogram of the ages of the resulting change points, where for analyses with two change points blue marks the older and green the younger of the two change points, with red representing analyses for which only one change point resulted. The conservative scenario of 1-h errors assigned to LOD values without known uncertainties yields a shallow mean slope indicating a resonance LOD value of between 18 and 20 h (Extended Data Fig. 1). The change points at ~2 and 1.2 Ga in our analysis (Fig. 2) therefore seem very robust, even when such attentional sources of potential uncertainty are considered. Overall, our statistical analysis reveals that two change points seem evident using the current dataset, but our results still need to be treated with caution and more data are urgently needed to confirm our conclusions.

Data availability

All of the data are available within the manuscript or its supplementary materials. The LOD compilation is available at https://doi.org/10.57760/sciencedb.08127.

Code availability

The MATLAB algorithm findchangepts is available at https://de.mathworks.com/help/signal/ref/findchangepts.html. Code to convert measured Milankovitch periods of precession and/or obliquity into LOD and Earth–Moon distance, modified from that of ref. 21, is available at https://doi.org/10.57760/sciencedb.08127.

References

23. Walker, J. C. G. & Zahnle, K. J. Lunar nodal tide and distance to the Moon during the Precambrian. *Nature* **320**, 600–602 (1986).
24. Lantink, M. L., Davies, J. H. F. L., Ovtcharova, M. & Hilgen, F. J. Milankovitch cycles in banded iron formations constrain the Earth–Moon system 2.46 billion years ago. *Proc. Natl Acad. Sci. USA* **119**, e2117146119 (2022).
25. Rodrigues, P. O. C., Hinnov, L. A. & Franco, D. R. A new appraisal of depositional cyclicity in the Neoarchean-Paleoproterozoic Dales Gorge Member (Brockman Iron Formation, Hamersley Basin, Australia). *Precambrian Res.* **328**, 27–47 (2019).
26. Cheng, D. et al. An astronomically calibrated stratigraphy of the Mesoproterozoic Hongshuizhuang Formation, North China: implications for pre-Phanerozoic changes in Milankovitch orbital parameters. *J. Asian Earth Sci.* **199**, 104408 (2020).
27. Grotzinger, J. Cyclicity and paleoenvironmental dynamics, Rocknest platform, northwest Canada. *GSA Bull.* **97**, 1208–1231 (1986).
28. Grotzinger, J. P. Upward shallowing platform cycles: a response to 2.2 billion years of low-amplitude, high-frequency (Milankovitch band) sea level oscillations. *Paleoceanography* **1**, 403–416 (1986).

29. Hinnov, L. A. Astronomical metronome of geological consequence. *Proc. Natl Acad. Sci. USA* **115**, 6104–6106 (2018).
30. Killick, R., Fearnhead, P. & Eckley, I. A. Optimal detection of changepoints with a linear computational cost. *J. Am. Stat. Assoc.* **107**, 1590–1598 (2012).
31. Lavielle, M. Using penalized contrasts for the change-point problem. *Signal Process.* **85**, 1501–1510 (2005).
32. Hofmann, A., Dirks, P. H. G. M. & Jelsma, H. A. Shallowing-upward carbonate cycles in the Belingwe Greenstone Belt, Zimbabwe: a record of archean sea-level oscillations. *J. Sediment. Res.* **74**, 64–81 (2004).
33. Pannella, G. Precambrian stromatolites as paleontological clocks. In *Proc. 24th International Geological Congress* 50–57 (Ed Gill, J. E.) (International Geological Congress, 1972).
34. Pannella, G. Paleontological evidence on the Earth's rotational history since early Precambrian. *Astrophys. Space Sci.* **16**, 212–237 (1972).
35. Liu, G. et al. Cyclostratigraphic calibration of the ca. 1.56 Ga carbon isotope excursion and oxygenation event recorded in the Gaoyuzhuang Formation, North China. *Glob. Planet. Change* **216**, 103916 (2022).
36. Zhang, S. et al. Orbital forcing of climate 1.4 billion years ago. *Proc. Natl Acad. Sci. USA* **112**, 1406–1413 (2015).
37. Mitchell, R. N., Kirscher, U., Kunzmann, M., Liu, Y. & Cox, G. M. Gulf of Nuna: astrochronologic correlation of a Mesoproterozoic oceanic euxinic event. *Geology* **49**, 25–29 (2021).
38. Vanyo, J. & Awramik, S. Stromatolites and Earth–Sun–Moon dynamics. *Precambrian Res.* **29**, 121–142 (1985).
39. Bao, X. et al. Cyclostratigraphic constraints on the duration of the Datangpo Formation and the onset age of the Nantuo (Marinoan) glaciation in South China. *Earth Planet. Sci. Lett.* **483**, 52–63 (2018).
40. Gong, Z. Cyclostratigraphy of the Cryogenian Fiq Formation, Oman and its implications for the age of the Marinoan glaciation. *Glob. Planet. Change* **204**, 103584 (2021).
41. Li, H. et al. Astrochronologic calibration of the Shuram carbon isotope excursion with new data from South China. *Glob. Planet. Change* **209**, 103749 (2022).
42. Gong, Z., Kodama, K. P. & Li, Y.-X. Paleomagnetism and rock magnetic cyclostratigraphy of the Ediacaran Doushantuo Formation, South China: constraints on the remagnetization mechanism and the encoding process of Milankovitch cycles. *Palaeogeogr. Palaeoclimatol. Palaeoecol.* **528**, 232–246 (2019).
43. Gong, Z., Kodama, K. P. & Li, Y.-X. Rock magnetic cyclostratigraphy of the Doushantuo Formation, South China and its implications for the duration of the Shuram carbon isotope excursion. *Precambrian Res.* **289**, 62–74 (2017).

Acknowledgements

R.N.M. was supported by a National Natural Science Foundation of China grant (number 41888101) and an Institute of Geology and Geophysics, Chinese Academy of Sciences Key Research Program grant (number IGGCAS-201905). X. Bao kindly helped to modify the code of ref. 21.

Author contributions

R.N.M. conceived of the idea, collected the data and wrote the manuscript. U.K. performed the statistical analyses with input from R.N.M. Both authors interpreted the data.

Competing interests

The authors declare no competing interests.

Additional information

Extended data is available for this paper at https://doi.org/10.1038/s41561-023-01202-6.

Supplementary information The online version contains supplementary material available at https://doi.org/10.1038/s41561-023-01202-6.

Correspondence and requests for materials should be addressed to Ross N. Mitchell.

Peer review information *Nature Geoscience* thanks Yonggang Liu and David Waltham for their contribution to the peer review of this work. Primary Handling Editors: Tamara Goldin and Rebecca Neely, in collaboration with the *Nature Geoscience* team.

https://doi.org/10.1038/s41561-023-01202-6

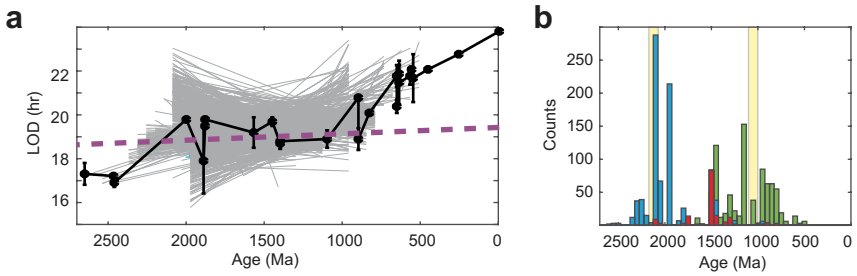

Extended Data Fig. 1 | Statistical analysis of length of day (LOD) evolution. An analysis was conducted where a 1 hr error was assigned to LOD estimates without known uncertainties. **a**, The original LOD data (black) and 1,000 re-samplings and associated repetitions of the linear regression of the middle interval from change-point analysis (grey lines). The resulting slope of the mean regression line through point 1500 Ma and 19 hours is shown (dashed purple). **b**, Histograms of resulting change points where blue (green) refers to older (younger) change points in analyses where 2 change points resulted. Red shows change points where only one was obtained from the analysis. The vertical yellow bars are the dominant ages of the two change points, consistent with our analysis in Fig. 2.

 https://doi.org/10.1038/s41561-023-01202-6

Extended Data Table 1 | Precambrian LOD constraints

Age (Ma)	Rock unit, geologic province	LOD (hr)	Uncertainty (hr)	Method	Reference
2650	Cheshire Fm, Zimbabwe	17.3	0.5	cyclostratigraphy	32
2465	Dales Gorge Member, Pilbara	17.2	0.1	cyclostratigraphy	19,25
2460	Joffre Member, Pilbara	16.9	0.2	cyclostratigraphy	22
2000	Great Slave Supergroup, Slave	19.8	–	stromatolites	33
1890	Rocknest Fm, Slave	17.9	–	cyclostratigraphy*	27
1880	Gunflint Fm, Superior	19.5	0.1	stromatolites	34
1880	Biwabik Iron Fm, Superior	19.8	–	stromatolites	33
1560	Gaoyuzhuang Fm, North China	19.2	0.7	cyclostratigraphy	35
1450	Hongshuizhuang Fm, North China	19.7	0.2	cyclostratigraphy	26
1400	Xiamaling Fm, North China	18.7	0.25	cyclostratigraphy	36
1400	Velkerri Fm, North Australia	18.8	–	cyclostratigraphy	37
1100	Nanfen Fm, North China	18.9	0.4	cyclostratigraphy	21
900	Big Cottonwood Fm, Laurentia	20.8	–	tidal rhythmites	11
900	Big Cottonwood Fm, Laurentia	18.9	0.5	tidal rhythmites	10
830	Bitter Springs Fm, Australia	20.1	–	stromatolites	38
655	Datangpo Fm, South China	21.8	0.5	cyclostratigraphy	39
655	Datangpo Fm, South China	20.4	0.3	cyclostratigraphy	19
640	Elatina Fm, Australia	21.9	0.4	tidal rhythmites	9
640	Fiq Fm, Oman	21.5	1	cyclostratigraphy	40
570	Doushantuo Fm, South China	21.8	0.4	cyclostratigraphy	41
560	Doushantuo Fm, South China	22.1	0.1	cyclostratigraphy	42
550	Doushantuo Fm, South China	21.7	1.1	cyclostratigraphy	43

*Modern cyclostratigraphic methods not used (see Methods for details).